A novel mutation, outside of the candidate region for diagnosis, in the inverted formin 2 gene can cause focal segmental glomerulosclerosis

Maria Sanchez-Ares[1], Marina Garcia-Vidal[1], Espinosa-Estevez Antucho[1], Pardo Julio[2], Vazquez-Martul Eduardo[3], Xose M. Lens[1,4] and Miguel A. Garcia-Gonzalez[1]

[1]*Laboratory of Nephrology, Sanitary Research Institute (IDIS), Santiago de Compostela, Spain;* [2]*Department of Neurology, University Clinical Hospital (CHUS), SERGAS, Santiago de Compostela, Spain and* [3]*Anatomy Pathology Unit, Universitary Hospital, SERGAS, La Coruña, Spain*

Focal and segmental glomerulosclerosis (FSGS) is a histological pattern that has several etiologies, including genetics. The autosomal dominant form of FSGS is a heterogenic disease caused by mutations within three known genes: α-actinin 4 (*ACTN4*), canonical transient receptor potential 6 (*TRPC6*), and the inverted formin 2 (*INF2*) gene. More recently, *INF2* mutations have also been attributed to Charcot–Marie–Tooth neuropathy associated with FSGS. Here we performed direct sequencing, histological characterization, and functional studies in a cohort of families with autosomal dominant FSGS. We detected a novel mutation in exon 6 of the *INF2* gene outside of the exon 2–4 candidate region used for rapid diagnosis of autosomal dominant FSGS. This new mutation is predicted to alter a highly conserved amino-acid residue within the 17th α-helix of the diaphanous inhibitory domain of the protein. A long-term follow-up of this family indicated that all patients were diagnosed in adulthood, as opposed to early childhood, and progression to end-stage renal disease was at different times without clinical or electrodiagnostic evidence of neuropathy. Thus, this novel mutation in *INF2* linked to nonsyndromic FSGS indicates the necessity for full gene sequencing if no mutation is found in the current rapid-screen region of the gene.

Kidney International (2012) **83,** 153–159; doi:10.1038/ki.2012.325; published online 12 September 2012

KEYWORDS: diagnosis; focal segmental glomerulosclerosis; INFZ; mutation

Correspondence: *Maria Sanchez-Ares, Laboratory of Nephrology, Sanitary Research Institute, University Clinical Hospital, Santiago de Compostela, Spain. E-mail: maria.sanchez.ares@gmail.com or Miguel A. Garcia-Gonzalez, Laboratory of Nephrology, Sanitary Research Institute (IDIS) or Department of Neurology, University Clinical Hospital (CHUS), SERGAS, Santiago de Compostela, Spain. E-mail: miguel.garcia.gonzalez@sergas.es*

[4]Deceased

Received 1 February 2012; revised 24 July 2012; accepted 26 July 2012; published online 12 September 2012

Focal and segmental glomerulosclerosis (FSGS) is a histological pattern with different etiologies: primary (idiopathic) and secondary (i.e., those forms with known etiology).[1] The clinical pattern is characterized by heavy proteinuria, nephrotic syndrome, and the progressive loss of renal function, probably resulting in end-stage renal disease (ESRD) and renal replacement therapy. There has been a significant effort to classify both the etiology and pathology of FSGS; however, given its variable manifestations, physicians and researchers continue to struggle to understand the molecular mechanisms of the disease.[1–4]

Familial forms of FSGS account for up to 18% of all cases,[5] and the vast majority of these cases present with early childhood onset, whereas adult onset is very uncommon. The clinical spectrum is strongly influenced by the type of inheritance pattern. Indeed, autosomal recessive FSGS usually manifests as a severe phenotype with an early onset in neonates and young children, whereas the autosomal dominant FSGS (AD-FSGS) form is generally associated with a juvenile or adult onset. Several genes have been implicated with both autosomal recessive FSGS (*NPHS1*-encoding nephrin,[6] *NPHS2*-encoding podocin,[7] and *PLCE1*-encoding phosphoinositide-specific phospholipase C epsilon-1[8]) and AD-FSGS (*ACTN4*-encoding alpha-actinin 4[9] and *TRPC6*-encoding canonical transient receptor potential 6[10,11]).

Recently, Brown *et al.*[12] described a new locus for AD-FSGS on chromosome 14q32 that includes the inverted formin 2 (*INF2*) gene. To date, approximately 15% of screened AD-FSGS cases ($n = 194$) have been linked to mutations in *INF2*.[12–15] More recently, Boyer *et al.*[16] discovered that mutations in *INF2* are also responsible for Charcot–Marie–Tooth (CMT) neuropathy associated with FSGS. In both cases, mutations associated with the syndromic and nonsyndromic form of the disease are clustered in exons 2 to 4 of *INF2*, which encode the diaphanous inhibitory domain (DID). However, most syndromic mutations are localized between two putative DID-binding pockets coded by the 3′ end of exon 2 and 3, affecting DID function more severely than mutations related to the nonsyndromic disease. Exons 2–4 has been suggested as a rapid screening method

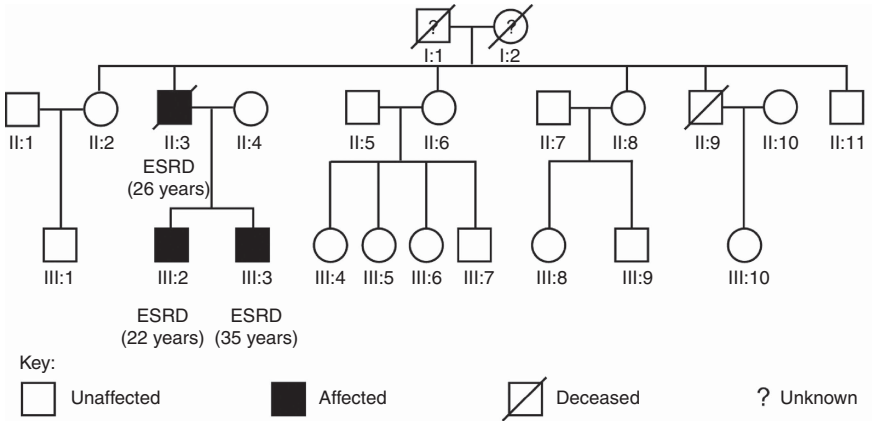

Figure 1 | Pedigree of the CHUS_FSGS-2 family with the mutation L245P. ESRD, end-stage renal disease.

for the diagnosis of both AD-FSGS[15] and CMT with glomerulopathy.[16] The DID domain allows INF2 to accelerate the polymerization and depolymerization of actin filaments and regulate specialized routes of protein targeting to the plasma membrane by forming protein complexes with Rho-GTPases, CDC42, and myelin and lymphocyte (MAL) protein, or MAL2 in podocytes and Schwann cells.[16–18] The main objective of this study is to conduct correlation studies in our cohort of Spanish AD-FSGS families. Although very little is known about INF2, the information provided by the mutational analysis in patients will help us improve our understanding of its functions and the pathogenesis of FSGS and CMT.

RESULTS

Clinical observations

We performed mutational analysis for AD-FSGS genes in five families (19 affected and 108 unaffected individuals) with a presumably autosomal dominant mode of inheritance of FSGS with two or more affected individuals in at least two generations.[15] Patients were classified following the inclusion criteria described below (Materials and Methods section). The age of diagnosis, maximum proteinuria levels, the presence of microhematuria and/or arterial hypertension, age at ESRD, and recurrence after transplant of affected individuals are presented in Supplementary Table S1 online. Initial mutational analyses for *ACTN4* and *TRPC6* were negative (sequence variants are shown in Supplementary Table S2 online). After the discovery by Brown *et al.*[12] that *INF2* mutations cause FSGS, we expanded our mutational analysis to this gene and identified a novel point mutation (L245P) in the CHUS_FSGS-2 family (see Supplementary Table S2 online for *INF2* sequence variants).

The proband of CHUS_FSGS-2 is a 21-year-old man (Figure 1 and Table 1, III:2) who had elevated blood urea, proteinuria in a nephrotic range, and microhematuria in a health maintenance visit; therefore, he was immediately referred to our hospital. Upon admission, he had an elevated blood pressure (170/110 mm Hg) with normal cardiothoracic and abdominal examinations. Blood tests showed abnormal levels of hemoglobin (10.7 g/dl), total plasma protein content (5.7 g/dl), albumin (3.3 g/dl), urea (125 mg/dl), creatinine (4.5 mg/dl), cholesterol (438 mg/dl), and triglycerides (253 mg/dl). Urinalysis confirmed a nephrotic-range proteinuria (7 g/l) and microhematuria. Renal ultrasound showed small kidneys (left, 80 mm; right, 85 mm) with hyperechogenic parenchyma.

On light microscopy, renal biopsy revealed FSGS with advanced glomerular damage. Several glomeruli already showed solidification of the entire tuft or global sclerosis. Severe tubulointerstitial injuries were also observed in areas of advanced tubular atrophy and interstitial fibrosis. Electron microscopy revealed extensive foot process effacement of podocytes without electron-dense deposits (data not shown).

We continued to follow-up the patient and observed that his renal function progressively declined. Within 6 months, he progressed to ESRD and underwent hemodialysis. A cadaveric renal transplant was performed at the age of 23. After a follow-up of 13 years post renal transplant (at the age of 36), there were no signs of FSGS recurrence. Given that INF2 mutations can be associated with CMT,[16] a complete clinical neurological evaluation was performed. The patient did not complain of numbness or weakness. Neurological examinations did not show signs of peripheral neuropathy, and *pes cavus* was not found. In addition to this, results of motor and sensory nerve conduction studies in the upper and lower limbs were normal.

Further analysis of the proband's family history revealed that his father and his brother (Figure 1, II:3 and III:3, respectively) also suffered from renal disease. The father was diagnosed at the age of 26 with advanced-stage renal failure, in addition to having symptoms of severe fatigue, polyuria, and high urea levels. Emergency hemodialysis was performed, but he died a few days later from technical complications.

Clinical records for the proband's brother (III:3) started at the age of 28 when elevated proteinuria was detected. He was referred to our hospital where a physical examination showed exclusively high blood pressure (155/80 mm Hg). Blood tests revealed hypercholesterolemia (293 mg/dl) and normal renal function (urea and creatinine levels of 31 and 1.2 mg/dl, respectively). A urinalysis showed normal

Table 1 | Phenotypes of affected patients in the CHUS_FSGS-2 family

	II:3	III:2	III:3
Age at diagnosis (years)	26	21	28
Maximal proteinuria (g/l)	N/A	7	7.8
Microhematuria	N/A	Yes	No
Arterial hypertension	N/A	Yes	Yes
Steroid response	Untreated	Untreated	Resistant
Cyclosporine response	Untreated	Untreated	Unresponsive
Age at ESRD (years)	26	22	35
Renal transplantation	No	Yes	Yes
Recurrence post transplantation	—	Not after 13 years	Not after 6 years

Abbreviations: ESRD, end-stage renal disease; N/A, not available.

urine sediment with elevated levels of proteinuria (7.8 g/l); the renal ultrasound was normal, and subsequently a renal biopsy was performed.

Light microscopic findings for patient III:3 demonstrated glomerular lesions characteristic of FSGS. Electron microscopy exhibited diffuse foot process effacement in all capillary loops. We also observed nonspecific ultrastructural changes in the mesangium and basal lamina, with irregular thickness of the subendothelial space, incipient widening, and duplication of the basal lamina. In some glomerular areas, a few granular and round particles were found in the mesangium and basal lamina (Figure 2). Immunofluorescent microscopy using glomerular markers detected focal and segmental deposits of C3 and mesangial IgM, with negative results for other immunoglobulins and complement fractions (data not shown).

Initially, a prolonged oral steroid treatment (1.5 mg/kg/day for 6 months) had no effect on his proteinuria, and his disease was considered steroid resistant. Subsequently, patient III:3 was treated with cyclosporine A (starting dose: 3 mg/kg bw/day, maintaining the trough level between 80 and 100 ng/ml) for 18 months; however, this treatment was also ineffective in reducing proteinuria levels. In addition, patient III:3 was treated with simvastatin for hypercholesterolemia and lisinopril for arterial hypertension. Lisinopril did not have an antiproteinuric effect. The patient's renal function progressively decreased, reaching ESRD 7 years after renal biopsy, and the patient started hemodialysis at the age of 35. Two years later, patient III:3 received a cadaveric renal transplant, and after 6 years of follow-up, his renal function remains normal with no signs of proteinuria. Neurological examinations and sensory and motor nerve conduction studies in upper and lower limbs were normal, without evidence of peripheral neuropathy.

Genetic analysis of *INF2*

From the AD-FSGS families in our cohort, we only found the disease associated with the novel *INF2* variant in one family (CHUS_FSGS-2). This mutation consists of a thymine-to-cytosine nucleotide substitution at exon 6 (c.734T>C), which is predicted to substitute a leucine residue for a proline residue in the INF2 protein (p.L245P, Figure 3a). To ensure

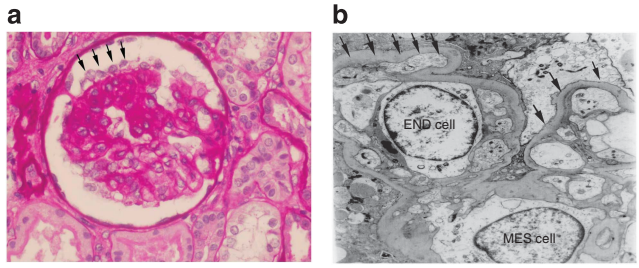

Figure 2 | Histopathological findings of the CHUS_FSGS-2 patient III:3. (**a**) Focal segmental distribution of glomerular lesions. The involved glomerulus shows a dense segmental scar. A monolayer of podocytes overlies the sclerotic segment. The sclerosis glomerular area is crowned by podocytes (arrows). Periodic acid Schiff original magnification ×400. (**b**) The ultrastructure study shows hyperplasic podocytes with foot effacement and continuous podocyte effacement (arrows). Subendothelial widening and irregularity without dense deposits are apparent. Original magnification ×7500. END cell, endothelial cell; MES cell, mesangial cell.

segregation with AD-FSGS, we confirmed that the L245P mutation was carried only by the affected family members and was not present in unaffected members (II:2, II:4, II:6, II:8, II:11, and III:10). In addition, this mutation was not identified in our control chromosomes or in public single-nucleotide polymorphism databases and the 1000 Genome Project. Supplementary Table S2 online shows a number of novel and previously described polymorphisms detected in our cohort of AD-FSGS families.

Molecular characterization and structural modeling of L245P

The mutation c.846T>C is located within the DID domain of INF2 (Figure 3b) and is an evolutionarily highly conserved residue between humans, chimpanzees, mice, and zebrafish INF2; human diaphanous-related formin 1; and mouse diaphanous-related formin 1 (mDia1) (Figure 3c). In addition, PolyPhen-2 predicts the pathogenicity of L245P to be '*Probably Damaging*,' with a score of 0.979 (sensitivity: 0.67; specificity: 0.94),[19] and Sorting Tolerant From Intolerant (SIFT) software found this mutation to be harmful, with a score of 0.03.[20]

Structural analysis predicts that the L245P mutation alters the architecture of the 17th α-helix (amino acids 239–264) of the DID domain by causing a turn point and forcing a bend of approximately 30° in the helix axis of this domain (Figure 4).

DISCUSSION

AD-FSGS is an uncommon form of familial FSGS that usually affects juvenile and adult patients, presenting as late-onset proteinuria and often leading to ESRD. Mutations in *ACTN4* and *TRPC6* have been associated with 7% of all screened cases of AD-FSGS.[5,9,10,21–23] Recently, mutations in exons 2 to 4 of the *INF2* gene have been linked to AD-FSGS nephropathy and CMT neuropathy associated with FSGS. Interestingly, many of these are recurrent mutations (15 novel and10 recurrent mutations) with variable renal and neurological phenotypes.[12–16] In this study, we describe the genetic screening and phenotypic analysis of a cohort of five families with

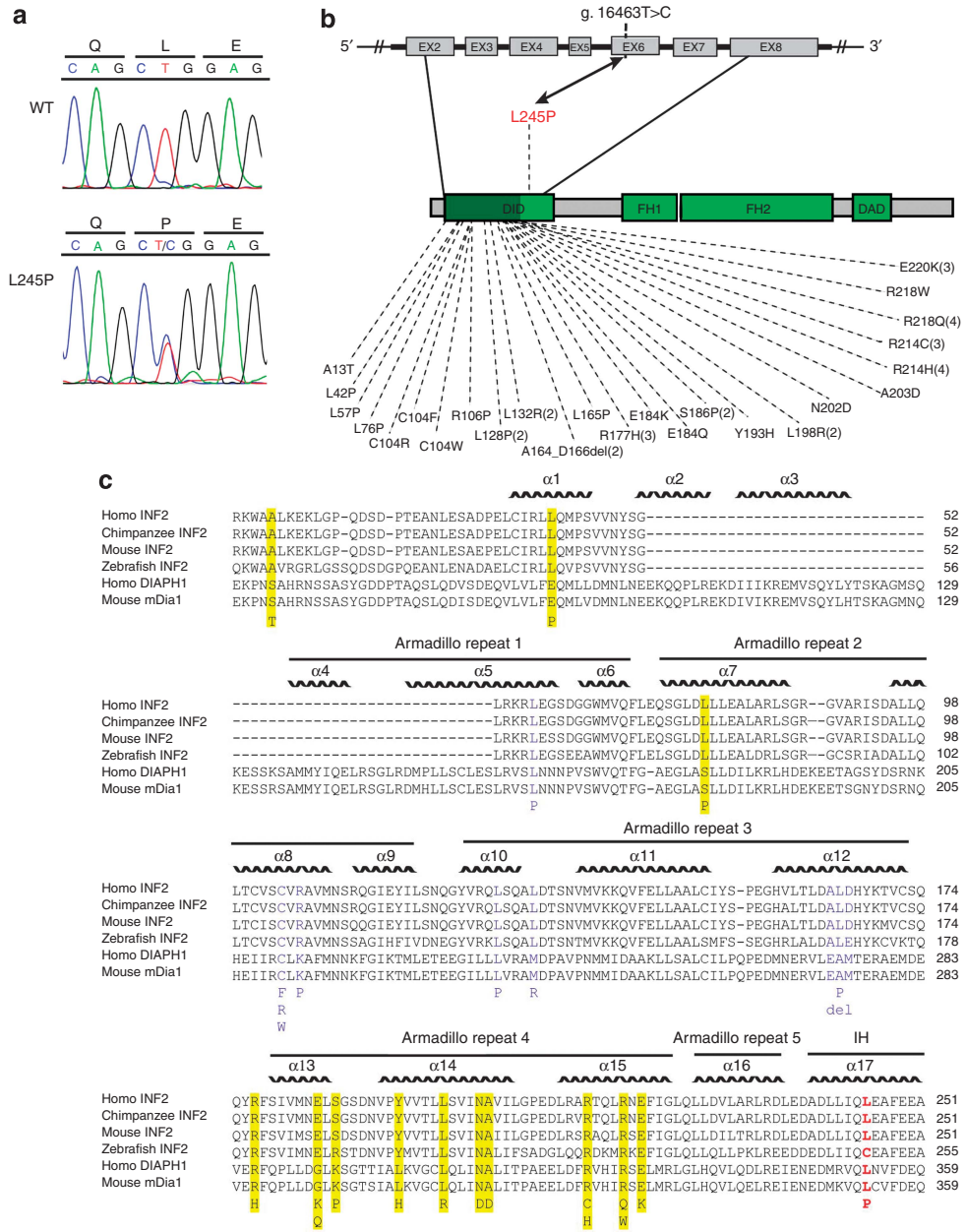

Figure 3 | Localization and evolutionary conservation of mutations in inverted formin 2 (*INF2*) gene. (**a**) Electropherogram showing the novel mutation (L245P) in exon 6 of *INF2* in the CHUS_FSGS-2 family. (**b**) Schematic representation showing exons 2–8 of the *INF2* gene and INF2 protein domain structure. The genomic and protein locations of L245P mutation are shown. All previously described *INF2* mutations fall into the diaphanous inhibitory domain (DID), codified by exons 2–4 (dark green). L245P is the first mutation found outside this hotspot. The number of recurrent mutational events is indicated in parentheses. (**c**) Alignment of the N-terminal sequences of human, chimpanzee, mouse, and zebrafish INF2; human diaphanous-related formin 1 (DIAPH1); and mouse diaphanous-related formin 1 (mDia1). INF2 mutations previously identified in patients with autosomal dominant focal and segmental glomerulosclerosis (AD-FSGS) alone are shown in yellow. INF2 mutations identified in patients with Charcot–Marie–Tooth (CMT) neuropathy associated with FSGS are shown in blue. The amino acid affected by the L245P mutation (red) is evolutionarily well conserved across species, as are the previously described mutations. The secondary protein structure of mDia1 is illustrated to localize the position of the mutations. Most of the mutations are in the α-helices. L245P is the first mutation described out of the armadillo repeats associated with FSGS alone and CMT neuropathy associated with FSGS. DAD, diaphanous autoregulatory domain; FH, formin homology; WT, wild type.

AD-FSGS. After negative mutational analysis for *ACTN4* and *TRPC6*, we found that one family carries a novel missense mutation (L245P) in exon 6 of *INF2*. We report the first *novel* mutation outside the candidate region for diagnosis of *INF2*, highlighting the need to sequence the entire gene if no mutations are found in exons 2 to 4. Furthermore, FSGS patients carrying the L245P mutation have no clinical or electrodiagnostic evidence of associated neuropathy, suggesting exon 6 as a region for nonsyndromic FSGS.

Mutations in autosomal recessive genes *NPHS1*, *NPHS2*, *CD2AP*, and *PLCE1* have been associated with severe FSGS, whereas mutations in *ACTN4*, *TRPC6*, and *INF2* have been

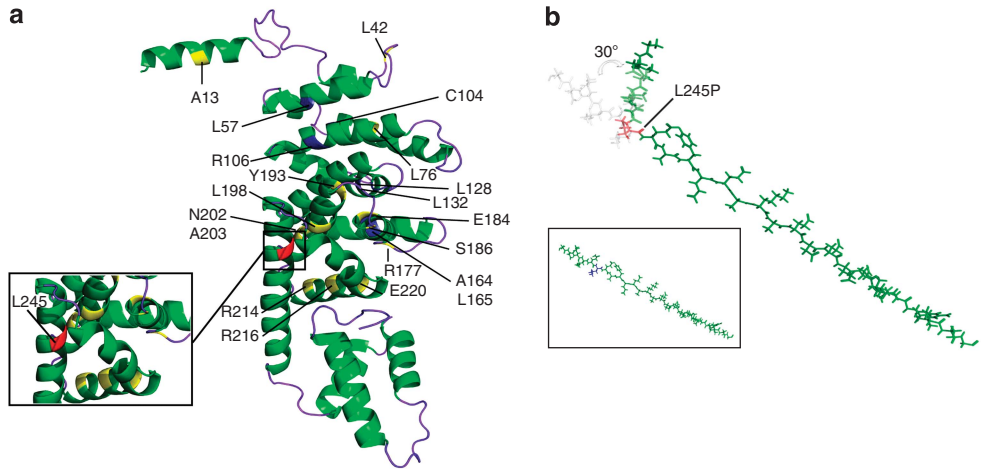

Figure 4 | Three-dimensional model of the diaphanous inhibitory domain (DID) of human inverted formin 2 (INF2). (**a**) View of the DID based on the structure of mouse diaphanous-related formin 1 (mDia1). Amino acids 1 through 330 of INF2 (corresponding to amino acids 46 through 440 of mDia1) are shown. The positions of the altered residues identified for autosomal dominant focal and segmental glomerulosclerosis (AD-FSGS) alone and Charcot–Marie–Tooth neuropathy associated with FSGS are presented in yellow and blue, respectively. The residue variant (L245P) identified in this study is shown in red, and it is located at 17th α-helix of the DID. (**b**) The proline substitution forces a bend of approximately 30° in the 17th α-helix of the DID. The wild-type 17th α-helix is boxed. When leucine is substituted for proline (red), the conformational structure of the wild-type helix (gray) is bent 30° (green) because proline cannot donate an amide hydrogen bond, and its side chain interferes sterically with the backbone of the preceding turn.

associated with a later-onset form of the disease.[24] All of the variants were found in podocyte genes that code for structural elements located in the glomerular slit diaphragm[25] and in proteins involved in the maintenance of the podocyte actin cytoskeleton. With the additional association of *INF2* mutations with AD-FSGS, the understanding of this disease has increased. Mutations in the *INF2* gene are major causes of familial AD-FSGS, with a prevalence of approximately 15% of all screened families in the world ($n = 195$, including the one described in this article). This prevalence is in clear contrast to the contribution of mutations in *TRPC6* (5.5%)[9–11,21–23] and *ACTN4* (1.5%).[5,9] A total of 69.3% ($n = 27$) of all *INF2* mutations previously identified cause nonsyndromic FSGS (exon 4: 61.5%, $n = 24$; exon 2: 7.7%, $n = 3$), whereas the remaining 30.7% result in syndromic FSGS (exon 2: 17.9%, $n = 7$; exon3: 12.8%, $n = 5$). Another distinctive characteristic of the *INF2* gene is its ability to inherit recurrent mutations (23.8%) when compared with the *ACTN4* and *TRPC6* genes (none), which is a unique characteristic among the AD-FSGS genes (Figure 3b).[12–16] Both aspects have led researchers to suggest that exons 2–4 of *INF2* are candidate regions for a rapid, noninvasive, and cost-effective mutational screening for diagnosing AD-FSGS linked to *INF2* gene.[14,15]

The INF2 protein is a member of the formin family of actin-regulatory proteins and has the following domains: a domain structure resembling an N-terminal DID[17]; formin homology 1 and 2 domains[26,27]; and a C-terminal WASP Homology 2 domain, which has the hallmarks of the diaphanous autoregulatory domain (DAD) present in other formins (Figure 3b).[17] The DID binds to the DAD, which autoinhibits the depolymerization but not the polymerization activity of INF2; this action is in contrast to other formins, where the DID/DAD binding inhibits both activities. Recently, Chhabra *et al.*[28] discovered that INF2 is predominantly localized in the endoplasmic reticulum and that mutations disrupting the DID/DAD interaction cause the endoplasmic reticulum to collapse because of the accumulation of actin filaments. When the DID/DAD interaction does not occur, actin polymerization is deregulated, which blocks the interaction of the INF2 protein with the formins of the DIA (diaphanous) group and alters the transport processes (transcytosis) mediated by the MAL protein and the MAL proteolipid protein 2 (MAL2).[29,30] Interestingly, all *INF2* mutations were found in exons coding for the DID.[12–16] Nature provides numerous examples of associations between mutations and phenotypes. Therefore, mutational screenings of affected individuals can help us generate databases of variations, which will be an invaluable tool to study the important functional domains. In particular, missense mutations are very important when studying specific residues and their critical functional properties.

The *INF2* gene was studied in our cohort after excluding *ACTN4* and *TRPC6*. Affected individuals in the CHUS_FSGS-2 family carried a nucleotide change in exon 6 that segregated with the disease. This change resulted in the substitution of the amino acid leucine to proline at position 245 (L245P) located within a highly conserved region on the 17th α-helix of the DID. In addition, the PolyPhen and SIFT software predicted that the change (L245P) would be highly pathogenic. Structurally, leucine and proline are two very different amino acids. The replacement of leucine residues with proline disturbs protein folding and commonly causes a turn point, resulting in a major conformational change.[31] Furthermore, proline is rarely found in α and/or β structures, as it would reduce the stability of such structures[32] because of

its α-N side chain, which can only act as a hydrogen bond acceptor.[31] Therefore, we inferred the impact of the L245P mutation, which would markedly alter the structure and possibly the function of the 17th α-helix of the DID domain (Figure 4b). The 17th α-helix is predicted to establish the initial weak interaction between the homolog of DID and Rho, permitting a second tighter interaction between them that then allows for the initialization of actin polymerization by the release of the DID/DAD complex.[16] Rose *et al.*[33] predicted that this α-helix constitutes the interdomain helix located between the armadillo repeats, the dimerization domain, and amino acids 347–377 of mDia1. In contrast, Otomo *et al.*[34] define this region as the second alpha helix of the fifth truncated armadillo repeat, amino acids 347–367 of mDia1. The vast majority of INF2 mutations are in α-helices (77% of the mutations described to date). Mutations within α-helices of the fourth armadillo repeat are only associated with FSGS, whereas mutations causing FSGS-associated CMT neuropathy are mostly located within α-helices of the second and third armadillo repeat.

The onset and severity of the phenotypes are extremely variable for individuals affected with FSGS in the CHUS_FSGS-2 family given that they share the same mutation. The proband III:2 and his father II:3 were diagnosed in adulthood (21 and 26 years of age, respectively) with advanced clinical manifestations of the disease and rapid progression to ESRD (1 and 6 months, respectively), suggesting an early onset of the disease. On the other hand, the proband's brother (III:3) had the adulthood-onset version of the disease (age of 28), with normal levels of creatinine and a moderate progression to ESRD (7 years later). This variability may be explained either by stochastic effects or genetic modifiers. The phenotypic presentation of many renal disorders is strongly influenced by the genetic environment. For example, other researchers and our group have shown that genetic interactions between dominant and recessive forms of polycystic kidney disease (PKD) can lead to a severe phenotype.[35] Therefore, we cannot rule out the fact that sequence variants in other FSGS genes or its downstream targets could modulate the severity and/or variability associated with the INF2 mutations. Despite this phenotypic variability, we provide further understanding of the disease and its relation to *INF2* function. Mutations in this new region of *INF2* are associated with nonsyndromic FSGS. Future studies should be directed at identifying new candidate genes of AD-FSGS to establish genotype–phenotype correlations in large FSGS cohorts. These studies would facilitate the understanding of the pathology and progression of the disease.

In conclusion, this study describes a mutational screening in a cohort of Spanish families with AD-FSGS. We identified a novel missense mutation (L245P) in exon 6 of the recently discovered disease-associated gene *INF2*. Although previous publications suggested exons 2 to 4 as the regions for diagnostic mutational screening, this study reveals that AD-FSGS mutations can be found beyond these exons. Because the location of the mutation in *INF2* may be related to disease manifestation (exons coding for the second and third DID armadillo repeats are associated with FSGS and CMT, whereas exons coding the fourth armadillo repeat are associated with FSGS alone), we describe a new protein region (17th α-helix of DID) responsible for AD-FSGS without neuropathy.

MATERIALS AND METHODS

Patients and data recruitment

The inclusion criteria are as follows: (i) renal biopsy demonstrating FSGS; (ii) substantial proteinuria; (iii) exclusion of secondary causes of FSGS; and (iv) exclusion of idiopatic or autosomal recessive FSGS (two or more affected individuals in one generation). Age at FSGS onset, course of glomerular disease, age at ESRD onset, kidney histology, and transplantation outcomes were obtained for each patient. The clinical characteristics are collected in Table 1. All participants were informed of the goal of the study, and consent was obtained in accordance with the local ethical committee (Galician Clinical Investigation Committee) and the Helsinki Declaration.

Electrodiagnostic testing

Nerve conduction studies were conducted using standard techniques [36] of surface stimulation and recording on a Nicolet Viking IV EMG equipment (Nicolet Biomedical Instruments, Madison, WI). Skin temperatures were maintained higher than 32.0 °C. Distal motor latency, F-wave latency, motor nerve conduction velocity, and compound motor action potential were measured in the median, ulnar, peroneal, and posterior tibial nerves. Sensory nerve conduction velocity and sensory nerve action potential were obtained in the median, ulnar, and sural nerves. Electromyography was performed in tibialis anterior and medial gastrocnemius muscles.

DNA isolation and mutation analysis

Genomic DNA was isolated from peripheral blood samples using the QIAmp DNA Mini Kit (Qiagen, Hilden, Germany) following the manufacturer's guidelines. We performed mutational analysis by PCR amplification of all exons and flanking regions of *ACTN4*, *TRPC6*, and *INF2* using the BioMix kit (Bioline, London, UK) and following the strategy described in Supplementary Table S3 online. Primers were designed with Primer3 (http://frodo.wi.mit.edu/primer3/). Sequencing reactions were performed using the BigDye Terminator v3.1 Cycle Sequencing Kit (Applied Biosystems, Warrington, UK). Sequencing was carried out using the ABI 3130xl Genetic Analyzer (Applied Biosystems) and analyzed by using the DNA Sequencing Analysis Software v5.2 (Applied Biosystems).

In silico prediction of amino-acid substitution L245P

The nonsynonymous sequence variants of genes were analyzed with the PolyPhen-2 software (http://genetics.bwh.harvard.edu/pph2/index.shtml)[19] and SIFT algorithm (http://sift.jcvi.org)[20] to predict the impact of the amino-acid substitution. Polyphen-2 calculates a Naïve Bayes posterior probability that any mutation is damaging by the representation of a score ranging from 0 to 1, as well as providing a qualitative damage based on the model's false-positive rate (benign, possibly damaging, or probably damaging). SIFT prediction is based on the degree of conservation of amino-acid residues in sequence alignments derived from closely related sequences providing a qualitative damage as well (tolerated or damaging).

Structural analysis for L245P mutation

Following the approach described by Brown *et al*,[12] we manipulated the DID domain model using the PyMol software (www.pymol.org) and identified the residues in mDia1 corresponding to our FSGS-novel mutation and the ones previously associated by others with the DID domain. In addition, we predicted the functional impact of our mutation constructing the wild-type and the mutant 17th α-helix of the DID domain by using the PyMol software as well.

Web resources

The following GenBank sequences (http://www.ncbi.nlm.nih.gov/Genbank/) served as reference files: NG_027684 for *INF2* genomic nucleotide position, NM_022489 for *INF2* cDNA position. UniProtKB (http://www.uniprot.org/help/uniprotkb, ID: Q27J81) and the Ensembl Genome Browser (http://www.ensembl.org, ID: ENSP00000376410) were used to determine the INF2 amino-acid position and ClustalW (http://www.ebi.ac.uk/clustalw/) for multiple sequence alignment.

DISCLOSURE

All the authors declared no competing interests.

ACKNOWLEDGMENTS

We acknowledge Perciliz L. Tan and Drs Sonia Eiras and Jana Alonso for paper editing. We thank Dr Martin Pollak for providing INF2 primer sequences. This work was supported by grants from Maria Barbeito Xunta de Galicia (MSA), Parga Pondal Xunta de Galicia (MAGG), Ministry of Science and Innovation, ISCIII, PI070164 (XML), and PI11/00690 (MAGG), Xunta de Galicia, INCITE-PXIB918238PR. We acknowledge the main contribution of this project to Dr Xosé Manuel Lens Neo (RIP), who devoted his life to family, friends, patients, and science until the last moment.

SUPPLEMENTARY MATERIAL

Table S1. Phenotypes of the affected patients of autosomal dominant focal and segmental glomerulosclerosis (AD-FSGS) families.
Table S2. Variants identified in α-actinin-4 (*ACTN4*), canonical transient receptor potential 6 (*TRPC6*), and inverted formin 2 (*INF2*) genes.
Table S3. Primer sequences for α-actinin-4 (*ACTN4*), canonical transient receptor potential 6 (*TRPC6*), and inverted formin 2 (*INF2*) genes.
Supplementary material is linked to the online version of the paper at http://www.nature.com/ki

REFERENCES

1. D'Agati VD. The spectrum of focal segmental glomerulosclerosis: new insights. *Curr Opin Nephrol Hypertens* 2008; **17**: 271–281.
2. Barisoni L, Schnaper HW, Kopp JB. A proposed taxonomy for the podocytopathies: a reassessment of the primary nephrotic diseases. *Clin J Am Soc Nephrol* 2007; **2**: 529–542.
3. Benoit G, Machuca E, Antignac C. Hereditary nephrotic syndrome: a systematic approach for genetic testing and a review of associated podocyte gene mutations. *Pediatr Nephrol* 2010; **25**: 1621–1632.
4. Pollak MR. Focal segmental glomerulosclerosis: recent advances. *Curr Opin Nephrol Hypertens* 2008; **17**: 138–142.
5. Weins A, Kenlan P, Herbert S *et al.* Mutational and biological analysis of alpha-actinin-4 in focal segmental glomerulosclerosis. *J Am Soc Nephrol* 2005; **16**: 3694–3701.
6. Kestila M, Lenkkeri U, Mannikko M *et al.* Positionally cloned gene for a novel glomerular protein—nephrin—is mutated in congenital nephrotic syndrome. *Mol Cell* 1998; **1**: 575–582.
7. Boute N, Gribouval O, Roselli S *et al.* NPHS2, encoding the glomerular protein podocin, is mutated in autosomal recessive steroid-resistant nephrotic syndrome. *Nat Genet* 2000; **24**: 349–354.
8. Hinkes B, Wiggins RC, Gbadegesin R *et al.* Positional cloning uncovers mutations in PLCE1 responsible for a nephrotic syndrome variant that may be reversible. *Nat Genet* 2006; **38**: 1397–1405.
9. Kaplan JM, Kim SH, North KN *et al.* Mutations in ACTN4, encoding alpha-actinin-4, cause familial focal segmental glomerulosclerosis. *Nat Genet* 2000; **24**: 251–256.
10. Reiser J, Polu KR, Moller CC *et al.* TRPC6 is a glomerular slit diaphragm-associated channel required for normal renal function. *Nat Genet* 2005; **37**: 739–744.
11. Winn MP, Conlon PJ, Lynn KL *et al.* A mutation in the TRPC6 cation channel causes familial focal segmental glomerulosclerosis. *Science* 2005; **308**: 1801–1804.
12. Brown EJ, Schlondorff JS, Becker DJ *et al.* Mutations in the formin gene INF2 cause focal segmental glomerulosclerosis. *Nat Genet* 2010; **42**: 72–76.
13. Lee HK, Han KH, Jung YH *et al.* Variable renal phenotype in a family with an INF2 mutation. *Pediatr Nephrol* 2010; **26**(1): 73–76.
14. Boyer O, Benoit G, Gribouval O *et al.* Mutations in INF2 are a major cause of autosomal dominant focal segmental glomerulosclerosis. *J Am Soc Nephrol* 2011; **22**: 239–245.
15. Gbadegesin RA, Lavin PJ, Hall G *et al.* Inverted formin 2 mutations with variable expression in patients with sporadic and hereditary focal and segmental glomeruloscerosis. *Kidney Int* 2011; **81**: 94–9.
16. Boyer O, Nevo F, Plaisier E *et al.* INF2 mutations in Charcot-Marie-Tooth disease with glomerulopathy. *N Engl J Med* 2011; **365**: 2377–2388.
17. Chhabra ES, Higgs HN.. INF2 Is a WASP homology 2 motif-containing formin that severs actin filaments and accelerates both polymerization and depolymerization. *J Biol Chem* 2006; **281**: 26754–26767.
18. Lammers M, Meyer S, Kuhlmann D *et al.* Specificity of interactions between mDia isoforms and Rho proteins. *J Biol Chem* 2008; **283**: 35236–35246.
19. Adzhubei IA, Schmidt S, Peshkin L *et al.* A method and server for predicting damaging missense mutations. *Nat Methods* 2010; **7**: 248–249.
20. Kumar P, Henikoff S, Ng PC.. Predicting the effects of coding non-synonymous variants on protein function using the SIFT algorithm. *Nat Protoc* 2009; **4**: 1073–1081.
21. Santin S, Ars E, Rossetti S *et al.* TRPC6 mutational analysis in a large cohort of patients with focal segmental glomerulosclerosis. *Nephrol Dial Transplant* 2009; **24**: 3089–3096.
22. Heeringa SF, Moller CC, Du J *et al.* A novel TRPC6 mutation that causes childhood FSGS. *PLoS One* 2009; **4**: e7771.
23. Zhu B, Chen N, Wang ZH *et al.* Identification and functional analysis of a novel TRPC6 mutation associated with late onset familial focal segmental glomerulosclerosis in Chinese patients. *Mutat Res* 2009; **664**: 84–90.
24. Pei Y.. INF2 is another piece of the jigsaw puzzle for FSGS. *J Am Soc Nephrol* 2011; **22**: 197–199.
25. Mundel P, Reiser J.. Proteinuria: an enzymatic disease of the podocyte? *Kidney Int* 2010; **77**: 571–580.
26. Higgs HN, Peterson KJ. Phylogenetic analysis of the formin homology 2 domain. *Mol Biol Cell* 2005; **16**: 1–13.
27. Pollard TD.. Regulation of actin filament assembly by Arp2/3 complex and formins. *Annu Rev Biophys Biomol Struct* 2007; **36**: 451–477.
28. Chhabra ES, Ramabhadran V, Gerber SA *et al.* INF2 is an endoplasmic reticulum-associated formin protein. *J Cell Sci* 2009; **122**: 1430–1440.
29. Andrés-Delgado L, Antón O, Madrid R *et al.* Formin INF2 regulates MAL-mediated transport of Lck to the plasma membrane of human T lymphocytes. *Blood* 2010; **116**: 5919–29.
30. Madrid R, Aranda JF, Rodriguez-Fraticelli AE *et al.* The formin INF2 regulates basolateral-to-apical transcytosis and lumen formation in association with Cdc42 and MAL2. *Dev Cell* 2010; **18**: 814–827.
31. Richardson JS, Richardson DC. Amino acid preferences for specific locations at the ends of alpha helices. *Science* 1988; **240**: 1648–1652.
32. Pace CN, Scholtz JM. A helix propensity scale based on experimental studies of peptides and proteins. *Biophys J* 1998; **75**: 422–427.
33. Rose R, Weyand M, Lammers M *et al.* Structural and mechanistic insights into the interaction between Rho and mammalian Dia. *Nature* 2005; **435**: 513–518.
34. Otomo T, Otomo C, Tomchick DR *et al.* Structural basis of Rho GTPase-mediated activation of the formin mDia1. *Mol Cell* 2005; **18**: 273–281.
35. Garcia-Gonzalez MA, Menezes LF, Piontek KB *et al.* Genetic interaction studies link autosomal dominant and recessive polycystic kidney disease in a common pathway. *Hum Mol Genet* 2007; **16**: 1940–1950.
36. Oh S. *Clinical Electromyography-Nerve Conduction Studies*, 2nd edn Williams & Wilkins: Baltimore, MD, 1993.